

Electron Thermal Transport Barrier and Magnetohydrodynamic Activity Observed in Tokamak Plasmas with Negative Central Shear

M. R. de Baar, G. M. D. Hogeweij, N. J. Lopes Cardozo, A. A. M. Oomens, and F. C. Schüller
FOM Instituut voor Plasmafysica "Rijnhuizen," Association EURATOM-FOM, P.O. Box 1207, 3430 BE
Nieuwegein, The Netherlands

(Received 30 October 1996; revised manuscript received 23 January 1997)

In the Rijnhuizen Tokamak Project, plasmas with steady-state negative central shear (NCS) are made with off-axis electron cyclotron heating. Shifting the power deposition by 2 mm results in a sharp transition of confinement. The good confinement branch features a transport barrier at the off-axis minimum of the safety factor (q), where $q \leq 3$, and two magnetohydrodynamic (MHD) instabilities, where one is localized at the off-axis minimum of q and one covers the entire NCS region. The low confinement branch has $q > 3$ everywhere, no transport barrier, and no MHD activity. [S0031-9007(97)03341-3]

PACS numbers: 52.25.Fi, 52.50.Gj, 52.55.Fa

Tokamaks [1] are toroidal devices in which hot plasmas are confined by means of magnetic fields. The plasma is characterized by the major radius of the torus (R_0) and the minor radius (a). External coils generate the dominant toroidal magnetic field (B_ϕ). A toroidal electric current in the plasma (I_p) adds a smaller poloidal component. The resulting helical field lines lie (to good approximation) on nested tori, which are characterized by their minor radius r or $\rho = r/a$. The safety factor q is a function of ρ . q and its derivative with respect to ρ , the magnetic shear $\hat{s} = (\rho/q)(\partial q/\partial \rho)$ play an important role in plasma stability. In standard tokamak operation the current density (j) is peaked on axis, leading to a q profile $q(\rho)$ with $\hat{s} > 0$ everywhere. Recently, tokamak plasmas with an induced off-axis minimum in q and a region of negative central shear (NCS) have gained much attention in view of their good plasma confinement. Strong peaking of the ion temperature (T_i) and the electron density (n_e) profiles leading to record values of the fusion performance have been reported from several devices [2–8]. The Rijnhuizen Tokamak Project (RTP) plasmas with steady-state NCS showed that the net energy transport was nearly zero in the core, which was shown to be caused by the canceling of diffusive and convective components of the heat flux [9].

The present paper concentrates on the observation of an electron thermal transport barrier and reports specific instabilities that can develop as a result of the NCS. Theoretical analyses have shown that the negative shear can stabilize the high- n ballooning mode, allowing higher values of the ratio of kinetic and magnetic pressure (β) [10]. However, other magnetohydrodynamic (MHD) modes can be destabilized, such as the infernal mode [11,12], an ideal pressure-driven MHD mode which requires $\hat{s} \approx 0$, or the double tearing mode [13,14]. Chu *et al.* [15] report the observation of the resistive interchange mode in NCS discharges with peaked pressure profiles.

In RTP [9], NCS can be reproduced by off-axis electron cyclotron heating (ECH) in discharges with $n_e > 3 \times 10^{19} \text{ m}^{-3}$, and $I_p < 80 \text{ kA}$. Power from a 110 GHz

gyrotron (second harmonic, X mode) is injected in the horizontal midplane from the low field side. The ECH pulse length is 150 ms. In the experiments described here, the power deposition was at $\rho_{\text{dep}} \approx 0.5$. The 350 kW absorbed ECH power exceeds the ohmic input power by a factor of 5 in the ECH phase. The off-axis heating leads to a steady-state hollow T_e profile with a corresponding hollow j profile and NCS. Measurements have been done with a multichannel radiometer and a 118-point single shot Thomson scattering system.

Figure 1 shows a series of Thomson scattering n_e and T_e profiles. The first T_e profile ($t = 149 \text{ ms}$) is obtained with ohmic dissipation only. ECH is switched on at $t = 150 \text{ ms}$. After 5 ms, a rapid increase of $T_e(\rho > 0.5)$ is observed. As a consequence, the current diffuses

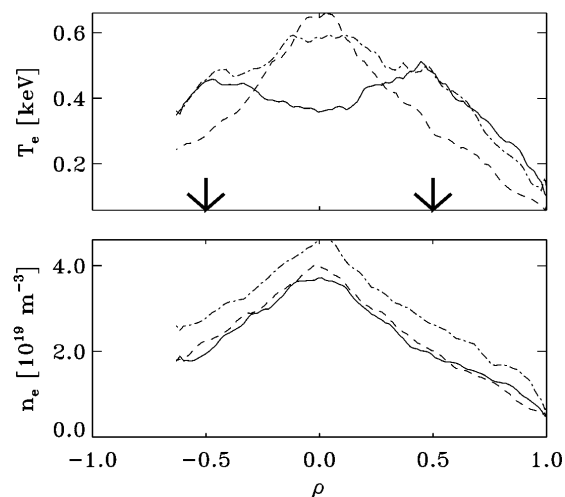


FIG. 1. Evolution of the T_e and n_e profile as measured with Thomson scattering in a series of nearly identical discharges with $q_a = 5.2$. ECH is switched on at $t = 150 \text{ ms}$. The arrows indicate ρ_{dep} . Shown are profiles measured at $t = 149 \text{ ms}$ (dashed line), $t = 155 \text{ ms}$ (dash-dotted line), and $t = 230 \text{ ms}$ (solid line). The shape of the n_e profile is hardly affected by the off-axis heating. The differences in top density are due to shot-to-shot variations, which are smaller than 10%.

outwards. The central current density decreases and, with it, the ohmic power density in the center of the plasma. For sufficiently high n_e , the electron-ion energy exchange can now beat the ohmic input, leading to a hollow T_e profile. The peakedness of the density profiles (see Fig. 1) is favorable for this process. Typically, after 50 ms, a new equilibrium is reached.

The final equilibrium can be in one of two classes with different confinement. In Fig. 2, the evolution of $T_e(0)$, as measured by the radiometer, is presented for seven discharges. Although the discharges all start from nearly the same state, they split into two branches after ≈ 30 ms. There is no correlation between the initial T_e and the final state of the discharge. The subtlety of the branching is illustrated by one discharge (dash-dotted line), which hesitates and then crosses over from the low to the high branch.

The current diffusion time is ≈ 20 ms, full current diffusion is established 50 ms after switch on of ECH. After this time the q profiles can be computed from $T_e(\rho)$, assuming neoclassical resistivity with a uniform distribution of the effective ion charge Z_{eff} . In these discharges, $Z_{\text{eff}} \approx 2$. In Fig. 3, $q(\rho)$ is plotted for an ohmic discharge, and for discharges in the low and high branch of confinement. In the high branch, a minimum of q goes just under 3, whereas in the low branch, $q = 3$ is not reached. The error bars are obtained by allowing the Z_{eff} profile to vary by 20% over the cross section, in accordance with previous measurements [16]. The shown q profiles are consistent with polarimeter data.

Figure 4 shows the electron pressure (p_e) profiles of two discharges in the different branches. Clearly visible is the steep gradient in p_e at $\rho = 0.5$ of the high branch; this region will be referred to as the transport barrier. It has a

width of ≈ 1.5 cm. Apart from the barrier, the gradients in p_e are similar, and the difference in confinement is fully determined by the presence or absence of the barrier. The energy confinement time in the low and in the high branch are $\tau_E^L = 1.4$ ms and $\tau_E^H = 1.7$ ms, respectively.

Corroborating evidence for the existence of a transport barrier is obtained with the ECH system in modulation mode, heating a plasma that crosses over from the low to the high branch of confinement. Heat pulses propagate through the plasma, and their amplitude and phase relative to the ECH pulses can be related to the electron heat transport. In Fig. 5, the dashed line depicts the modulation of the ECH power and trace (a) $T_e(0)$. Between $t = 165$ ms and 170 ms, the discharge crosses over to the high branch. Traces (b) and (c) represent $T_e(\rho_{\text{dep}})$ and $T_e(\rho > \rho_{\text{bar}})$, respectively, in which ρ_{bar} is the position of the barrier. The amplitude of the modulated $T_e(\rho_{\text{dep}})$ increases significantly when the transition from the low to the high branch occurs. The T_e modulation outside ρ_{bar} slightly decreases. These observations are consistent with the formation of a transport barrier just outside ρ_{dep} .

While none of the discharges in the low branch of confinement show MHD activity, many in the high branch do. In Fig. 6(a), $T_e(t)$ at ρ_{dep} is shown. An oscillation with a period of 1 ms is observed. This oscillation has a constant amplitude over 30 periods. During this time, the central T_e shows no activity. The rise time of the oscillation is typically 800 μ s, and the rapid decrease occurs in 200 μ s. We shall refer to this fast decrease as a minor crash. Figure 7(a) shows the T_e profiles just before and right after the minor crash. Note that the minor crash is a phenomenon that is localized near ρ_{dep} , where q reaches an off-axis minimum with $q < 3$.

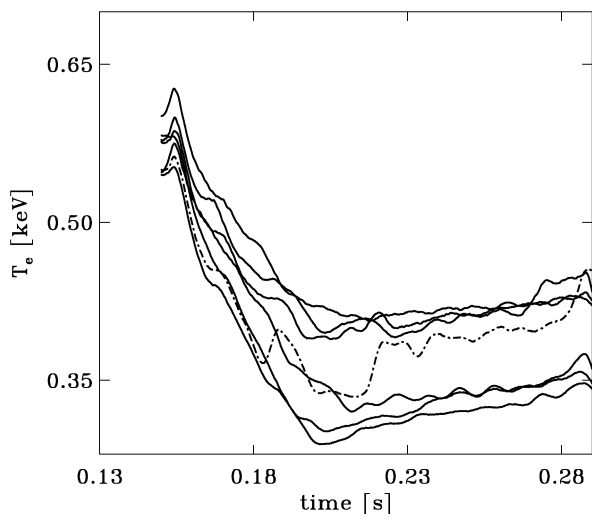


FIG. 2. Evolution of $T_e(0)$ as measured by ECE in seven nearly identical discharges after switch on of ECH at $t = 150$ ms, showing the two levels of confinement. The subtlety of the distinction between these levels is illustrated by one discharge (dash-dotted line) that crosses over from the low to the high branch.

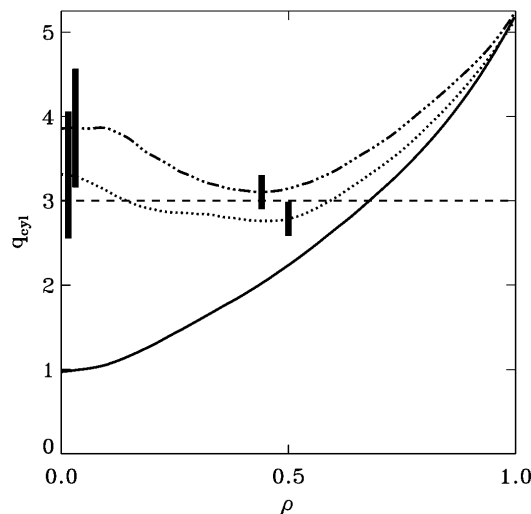


FIG. 3. Safety factor of high confinement discharge (dotted line). Note that $q(\rho_{\text{dep}}) < 3$. The q profile of a discharge of the low confinement branch is shown (dash-dotted line) for comparison. The minimal value of q in this case is 3.1. In the solid line, the q profile in the ohmic phase of the discharge is shown. The error bars are presented for q_0 and the region around q_{min} .

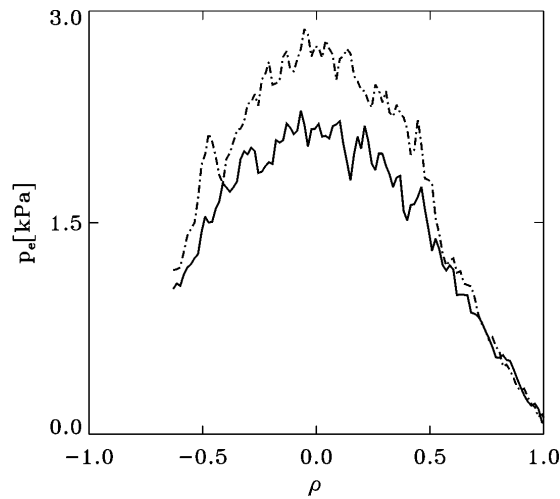


FIG. 4. Pressure profiles of a discharge in the low branch (full line) and a discharge in the high branch (dash-dotted line). Note that both profiles have the same gradients, except for the region around $\rho = 0.5$. Here a transport barrier has formed in the high branch.

The period of oscillations with constant amplitude ends when, at $t = 252$ ms, the amplitude of the oscillation at ρ_{dep} starts to grow. It reaches its maximum value at $t = 254$ ms, when a sudden increase in central T_e is observed [see Fig. 6(b)]. Then the amplitude of the oscillation at ρ_{dep} decreases again. The central T_e decreases in 5 ms, after which the sequence repeats itself. The sudden increase of the central T_e will be referred to as the major crash. Figure 7(b) shows the T_e profiles just before and just after the major crash. In this event, the entire central part ($\rho < \rho_{\text{dep}}$) of the plasma column is affected, while the outer region ($\rho > \rho_{\text{dep}}$) is not affected.

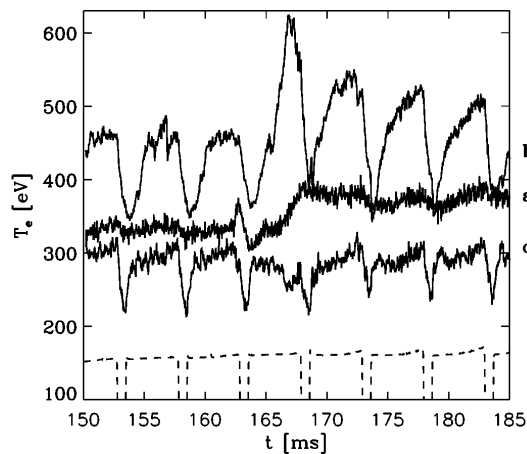


FIG. 5. ECH modulation sequence (dashed line) and $T_e(0)$ (a), $T_e(\rho_{\text{dep}})$ (b), and $T_e(\rho > \rho_{\text{bar}})$ (c). The ECH was switched on at $t = 110$ ms. Between $t = 165$ and 170 ms, the discharge crosses over to the high branch. The formation of the barrier is evidenced by the fact that inside ρ_{dep} the amplitude of the modulation in T_e significantly increases, whereas outside the barrier the amplitude of the modulation in T_e decreases.

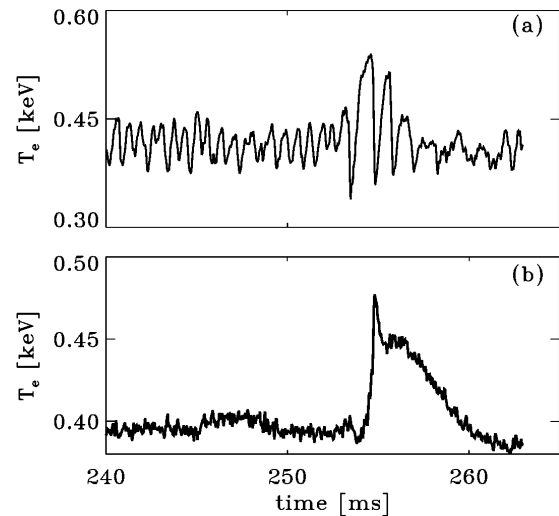


FIG. 6. $T_e(\rho_{\text{dep}})$ (a) and $T_e(0)$ (b) showing many minor crashes and one major crash (see text).

The high branch q profile plotted in Fig. 3 was measured 1 ms before the major crash and between two minor crashes. A double tearing mode involving the two $q = 3$ surfaces is a likely candidate for the cause of this crash, but the conditions are also favorable for the resistive interchange mode. On the basis of the present data we cannot decide between these two. The infernal mode is less likely because, at $\beta_{\text{pol}} \approx 0.5$, the pressure is insufficient to drive this mode unstable. The explanation of the major crash remains open until more detailed knowledge on the evolution of the plasma parameters is available. Note that, while in the minor crash, the energy of the off-axis T_e maximum is mainly transported out to larger ρ ; in the major crash, the energy is transported inward, leaving the plasma outside ρ_{dep} unaffected. It should be noted that, in both cases, the Mirnov coils do not show any signal

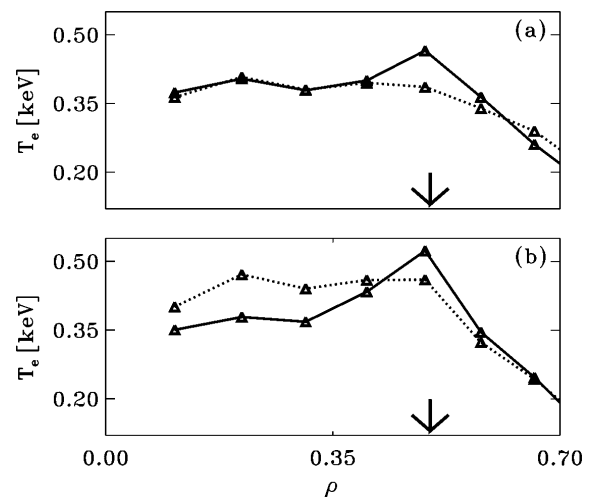


FIG. 7. $T_e(r)$ just before (solid line) and after (dotted line) a minor crash (a) and a major crash (b). The minor crash affects only the region near ρ_{dep} , whereas the major crash affects the whole central ($\rho < \rho_{\text{dep}}$) plasma.

in relation to the modes observed, nor could they be expected to do so. The coils are positioned rather far from the plasma, and the magnetic perturbations under observation have a high mode number ($m \geq 3$) and are localized within $r = 8$ cm. The five camera soft x-ray tomography system clearly observed the activity, but could not resolve the mode structure.

The difference in confinement between the two branches is due to the presence or absence of the transport barrier near ρ_{dep} . Two pertinent questions are (1) why does the transition occur, and (2) is the transport barrier associated with the deposition radius or rather with the position of the $q = 3$ surface? There is a single experimental answer to both questions. The one macroscopic plasma parameter that appears to be decisive for the sharp transition is the precise location of the power deposition, here defined as the radius of cold resonance: In the discharges in the high confinement branch, ρ_{dep} is marginally smaller than in those with low confinement (see Fig. 8). The transition occurs sharply for a variation of ρ_{dep} by 0.01 (i.e., 0.2 cm in the plasma). Note that this is much less than the width of either the barrier or the power deposition, which rules out the possibility that the barrier is present in both confinement modes. The discrete step in confinement brought about by this small change of ρ_{dep} indicates that the transport barrier is associated with an intrinsic plasma property, rather than the power deposition itself. The only plasma property that has such a discrete localization is the position of the $q = 3$ surface. Corroboration of this interpretation was obtained in later experiments, in which ρ_{dep} was kept constant while I_p was varied. In these experiments a similarly sharp step of confinement was observed for a variation of I_p of $< 2\%$.

The answer to the question as to why there are two discrete levels of confinement in the equilibrium

situation is then that deposition just inside the barrier leads to a more pronounced off-axis maximum in T_e , which prevents the minimum of q from going above 3. Conversely, deposition a little further out allows the minimum of q to rise above 3, in which case the transport barrier disappears altogether, with a further rise of q as a consequence. Hence, the paradoxical situation presents itself, that the MHD activity develops only in the high confinement branch precisely because of the better confinement. The MHD activity does not destroy the good confinement, but it does prevent the T_e and j profiles from developing more strongly pronounced off-axis maxima.

In conclusion, the shape of the q profile with an off-axis minimum close to $q = 3$ is the cause of the observed phenomena. The question remains when this situation is reached. At the start of the ECH the deposition is well inside the $q = 3$ surface. In the first few ms, all discharges develop in the same way. In the experiments shown in Fig. 2 there are some trivial differences due to the small differences in ρ_{dep} ; in the experiments in which ρ_{dep} was fixed while I_p was varied, these differences do not occur. At $t \approx 165$ ms, there is a hitch in the evolution. According to current diffusion calculations, at this moment the q profile is flat inside ρ_{dep} . The high and low branches separate some time after this hitch. A detailed analysis of this phase, which should reveal when the transport barrier is formed, will be given in a forthcoming paper.

Dr. A. Montvai, Dr. H. Goedbloed, Dr. T. Schep, Dr. J. Rem, and Dr. E. Westerhof are acknowledged for stimulating discussions, and the RTP team for machine and diagnostic operation. This work was done under the Euratom-FOM association agreement with financial support from NWO and Euratom.

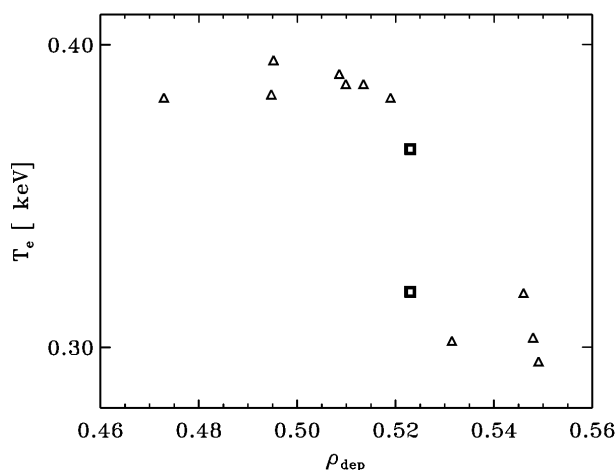


FIG. 8. Discharges in the high [$T_e(0) \approx 0.4$ keV] and low [$T_e(0) \approx 0.3$ keV] branch of confinement are separated by ρ_{dep} . The sharp transition corresponds to a difference of ρ_{dep} of 0.01. The discharge that crosses over sits exactly at this transition (squares).

- [1] J. A. Wesson, *Tokamaks*, The Oxford Engineering Science Series (Clarendon Press, Oxford, 1987), pp. 12–13.
- [2] E. J. Straight *et al.*, Phys. Rev. Lett. **75**, 4421 (1995).
- [3] B. W. Rice *et al.*, Plasma Phys. Control. Fusion **38**, 869–881 (1996).
- [4] F. M. Levinton *et al.*, Phys. Rev. Lett. **75**, 4417 (1995).
- [5] P. Smeulders *et al.*, Nucl. Fusion **35**, 225–242 (1995).
- [6] M. Hugon *et al.*, Nucl. Fusion **32**, 33 (1992).
- [7] X. Litaudon *et al.*, Report No. EUR-CEA-FC 1565, 1996 (to be published).
- [8] Y. Neyatani *et al.* (to be published).
- [9] G. M. D. Hogewij *et al.*, Phys. Rev. Lett. **76**, 632 (1996).
- [10] C. Kessel *et al.*, Phys. Rev. Lett. **72**, 1212 (1994).
- [11] T. Ozeki *et al.*, Nucl. Fusion **33**, 1025 (1993).
- [12] L. A. Charlton *et al.*, Nucl. Fusion **31**, 1835 (1991).
- [13] T. H. Stix, Phys. Rev. Lett. **36**, 521 (1976).
- [14] D. Biskamp, *Nonlinear Magnetohydrodynamics* (Cambridge University Press, Cambridge, England, 1993).
- [15] M. S. Chu *et al.*, Phys. Rev. Lett. **77**, 2710 (1996).
- [16] D. F. da Cruz, Ph.D. thesis, Rijksuniversiteit Utrecht, 1993 (unpublished).